Chinese Chemical Letters 32 (2021) 3558–3561

Contents lists available at ScienceDirect

Chinese Chemical Letters

journal homepage: www.elsevier.com/locate/cclet

Communication

X-site doping in ABX_3 triggers phase transition and higher T_c of the dielectric switch in perovskite

Youya Yu[a,b], Peizhi Huang[b], Yuzhen Wang[a,b], Zhixu Zhang[a], Tie Zhang[a], Yi Zhang[a,*], Dawei Fu[a,b,*]

[a] Ordered Matter Science Research Center,Jiangsu Key Laboratory for Science andApplications of Molecular Ferroelectrics, Southeast University, Nanjing 211189, China

[b] Institute for Science and Applications of Molecular Ferroelectrics, Key Laboratory of the Ministry of Education for Advanced Catalysis Materials, Zhejiang Normal University, Jinhua 321004, China

ARTICLE INFO

Article history:
Received 29 January 2021
Received in revised form 18 February 2021
Accepted 18 February 2021
Available online 22 February 2021

Keywords:
Dielectric switch
X-site doping
High-temperature
Phase transition
Molecule design

ABSTRACT

Material stability is always the key factor for applied materials especially the working environment that requires higher temperature sensitivity or temperature fluctuation range. In which, the stimulus-response perovskite materials are just sensitive to stability to ensure the accuracy and stability of the signals, in the applied devices of batteries and memory storage devices and so on. However, it is still a tremendous challenge to improve the stability of perovskite materials, and maintain reliability in the devices. Here, a novel $ABX_2X'_1$ (X-site doping in an ABX_3) compound [CEMP]-[$CdBr_2$(SCN)] (**1**, CEMP = 1-(2-chloro-ethyl)-1-methyl-piperidine) with remarkable high-temperature reversible dielectric switching behavior was proposed. The strategy of $[SCN]^-$doping in perovskite for improving the stability was successfully achieved. Meanwhile, the steric hindrance is increased while the energy barrier is also increased by replacing hydrogen with flexible groups, which leads to a high-temperature reversible phase transition. The new finding provides a new direction to enrich new applications and design ideas of perovskite materials. Especially the X-site strategy of doping or substitution in the ABX_3, it will promote ingenious and perfect experimental results in material synthesis and performance improvement by chemistry disciplines.

ABX_3 perovskites are the preferred core functional material for smart sensor and energy conversion, even multifunctional material in recent decades, especially in recent years [1–4]. As can be seen from the basic ABX_3 structure that each site of A, B or X can be designed and modified to improve the overall performance or trigger new functions by doping or substitution [5]. For example, methylamine lead iodide ($MAPbI_3$), the researchers carried out the doping and substitution in A, B or X sites, such as A = methylamine, B = Pb or Sn, X = halogen or doping halogen [6–8]. Regardless of the replacement or doping of the A/B/X site, significant progress has been made in the exploration of perovskite solar cells [9–11]. Similarly, such methods are not limited to the performance improvement and development of solar cells. In the field of sensor materials, it can still exhibit extensive controllable properties through A/B/X-site doping strategy. Halogen doping of chlorine, bromine and iodine is a common and effective method. The feasibility of a *pseudo*-halogen, such as $[SCN]^-$, has never been tried or proven. We summarized the doping regularity of ABX_3, and believe that $[SCN]^-$ can increase the flexibility of the structure by extending the distance between metals. It is very feasible to improve the structural phase transition and stability while the halogen with a poor coordination bond length keeps the stability of the basic unit structure [12,13]. It is the intense rigidity of the halogen poor coordination bond length that will cause the structure broken when the structural symmetry phase transition occurs. *Pseudo*-halogen doping is equivalent to a rigid-flexible combination mode, which can be considered as a perfect combination from the perspective of structural control [14,15]. Their physical properties materials could regulate by simple chemical modifications [16,17]. From the microscopic point of view, the flexible group is integrated into the stable inorganic framework, and the organic and inorganic perovskite material shows different states via thermal stimulation, which is an

* Corresponding authors at: Ordered Matter Science Research Center, Jiangsu Key Laboratory for Science andApplications of Molecular Ferroelectrics, Southeast University, Nanjing 211189, China.

E-mail addresses: yizhang1980@seu.edu.cn (Y. Zhang), dawei@seu.edu.cn (D. Fu).

https://doi.org/10.1016/j.cclet.2021.02.040

effective method to design the dielectric switch [18]. Researchers have found that a polyatomic bridging system is an end-to-end connection of two metal ions that can be multi-coordinated, which increases the degree of freedom of the A-position cation [19,20]. As previous work, a series of compounds with multi-atomic bridging ligand was reported, such as $[(CH_3)_nNH_{4-n}][Mn(N_3)_3]$ (n = 1–4) [21], $[(Me)_3N][Mn(HCOO)_3]$ [22]. They all show excellent dielectric switching properties, and $[SCN]^-$ ions, in particular, are thought to be more susceptible to phase transitions because they can form multiple structural types as bidentate ligands. As Chen reported, compared to $MAPbI_3$ materials, $MAPbI_{3-x}SCN_x$ has shown better device performance and stability [23]. Bearing these in mind, it is an effective strategy to heighten device stability and capability by adding $[SCN]^-$ ions to the perovskite precursor solution [24,25].

Based on the "*quasi*-spherical theory", ferroelectric materials can be effectively regulated and designed by introducing dipole components to reduce the symmetry of spherical molecules, which would restrain the crystallization of centrosymmetric structures [26–28]. As previously reported, a series of compounds with phase transition properties were obtained by combining methyl halides with quaternary ammonium salts so that the symmetry reduces, such as $[Me_3NCH_2Cl]MBr_3$ ($M = Cd^{II}$, Fe^{III}) [29,30], $[NH_3CH_2CH_2F]BiCl_3$ [31]. Therefore, it remains a significant challenge to achieve different types of phase transitions by controlling the movement of molecular dipoles [32–34].

Inspired by the above method, the X-site doping strategy in the $ABX_3$was shown in Scheme 1, whilethe reaction synthesis steps are shown in detail in Scheme S1 (Supporting information). We have found an exciting crystal material $[CEMP]_2[CdBr_4]$ (CEMP = 1-(2-chloro-ethyl)-1-methyl-piperidine) by introducing chloroethyl as a flexible group into the ammonium bromide at first, who shows no dielectric switching properties. After that, we synthesized [CEMP]-$[CdBr_2(SCN)]$ through combining 2-chloroethyl-1-methyl piperidine bromide with potassium thiocyanate and cadmium nitrate hexahydrate in proportion. As respected, the compound represents a reversible phase transition. Interestingly, different from the dielectric response materials completely dominant $[SCN]^-$ ions as bridging ligand materials, the compound replaces two of the bridging $[SCN]^-$ by bromine atom as a bridge and the other bromine atom as the terminal atoms to form five ligand. This is because the Cd atom is flexible to allow for a variety of geometrical configurations and coordination numbers, this type of structure depends on the size of the anion, shape, symmetry, and the proportion of Cd^{II} cation and $[SCN]^-$ ions [35]. Furthermore, the compound displays a sizeable thermal hysteresis about 27 K. The large thermal hysteresis attributes to the long time required for molecules to change from rotational motion to static state, and the thermal hysteresis temperature stays unchanged at each cycle which is in favor of time-delay mediadevices. In total, the work not only enriches the application of the organic and inorganic perovskite materials but provides a novel direction to upgrade the stability of hybrid materials by doping $[SCN]^-$ ions in perovskite compounds.

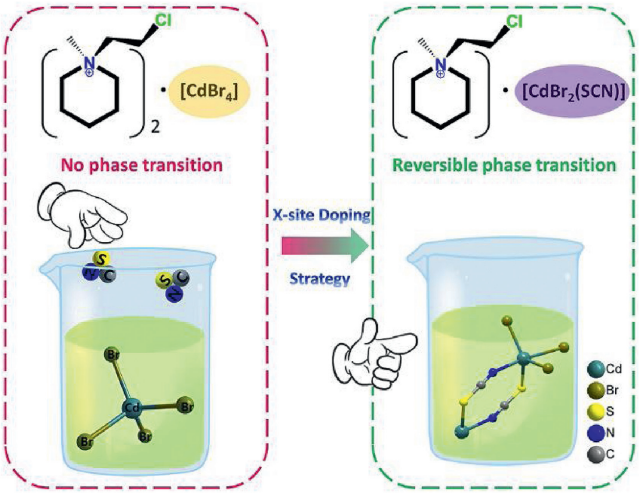

Scheme 1. X-site doping triggers phase switching.

Thermal analysis is regarded as one of the most effective strategies that can effectively achieve the transformation of physical and chemical properties. Differential scanning calorimetry measurement (DSC) was executed in a range of 250–350 K to prove the structural phase transition resulted from the altered temperature. As shown in Fig. 1, during the heating process there are obviously endothermic peaks appearing at 323 K (T_c) as well as one sharp exothermic peak at 296 K in the cooling procedure, which reveals a reversible phase transition at high temperature. The temperature above T_c is defined as the high-temperature phase (HTP), and the temperature range below T_c is the low-temperature phase (LTP).

The DSC curve is characterized by sharp peaks and wide thermal hysteresis of 27 K, which represents the first-order phase transition. By integrating on the DSC curve, the corresponding entropy changes (ΔS) are 10.9 J mol^{-1} K^{-1} for ΔS (T_c). Forasmuch the values of N (T_c) is calculated as 3.7 through the Boltzmann equation $\Delta S = R \ln(N)$, which tends to uncover that the phase transition has the characteristics of order-disorder. Thermogravimetric analysis (TGA) experiments were conducted in the temperature range of 300−1055 K for the sake of confirming that the phase transition at T_c is not owing to the decomposition of the crystal of **1**. The TGA curse (Fig. S1 in Supporting information) shows that the compound is stable up to 545 K, which further confirms that the crystal owns a stable high-temperature phase.

It is essential to make a thorough inquiry of the crystal structural transformation characteristics from LTP to HTP by using variable-temperature XRD in order to figure out the mechanism of the phase transitions. At 273 K (LTP), the cell parameters were $a = 8.9685(17)$ Å, $b = 16.181(3)$ Å, $c = 10.9641(17)$ Å, $\alpha = \gamma = 90°$, $\beta = 100.488(6)°$, $V = 1564.5(5)$ $Å^3$ and $Z = 4$. As can be seen from the stacking diagram (Figs. 2a and b), adjacent inorganic chains are parallel to each other, with organic cations occupying the middle channel. The structure of **1** consists of an infinite 1-D linear inorganic chain and $[CEMP]^+$ cation. The central cadmium atom has five anions, including one terminal bromine atom, and four bridging anions are, in turn, an S atom and an N atom from two $[SCN]^-$ ligands as well as two bromine atoms. The hexatomic ring of the $[CEMP]^+$ cation displays a chair-like state for structural stability (Fig. 2c). At 333 K (HTP), the cell parameters were $a = 9.0229(7)$ Å, $b = 16.2839(11)$ Å, $c = 10.9449(7)$ Å, $V = 1583.92(19)$ $Å^3$ and $Z = 4$, $\alpha = \gamma = 90°$, $\beta = 99.951(2)°$. Either at LTP or HTP, the

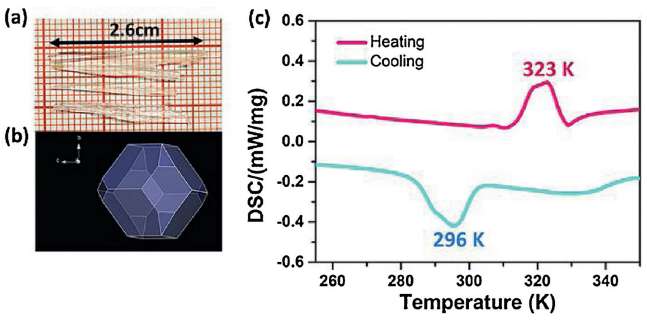

Fig. 1. (a) The as-grown crystals of **1** with a size of 26 × 3 × 2 mm^3. (b) Simulative single crystal shape of compound **1**. (c) DSC curves of **1** in the cooling-heating cycle.

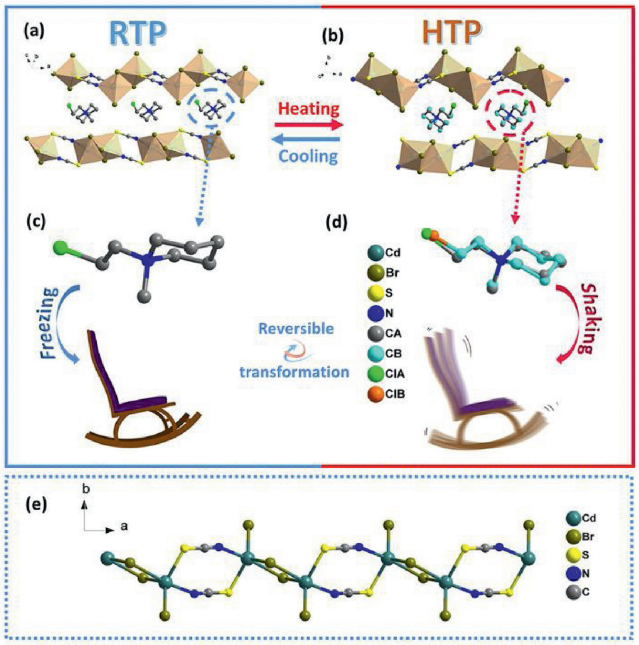

Fig. 2. Crystal-packing views of **1** at (a) LTP and (b) HTP. CEMP cation structural comparison of **1** between (c) LTP and (d) HTP. Chair-like CEMP cation displays a static state in the LTP and a rocking chair at HTP. The disordered CEMP cations are distinguished by different bond colors. The ordered carbon atoms show in the color gray while the disordered carbon atoms show in the color light blue. The ordered chlorine atom shows in green while the disordered chlorine atom shows in orange. All hydrogen atoms are omitted for clarity. (e) The metal chain at LTP.

complex **1** crystallize in the centrosymmetric space group $P2_1/m$ (No. 11), and the parameters do not vary much between the two phases. It means that the phase transition driving force is not sufficient enough to change the symmetry of space. Unlike the negligible change of cell parameters, the atomic vibrations of $[CEMP]^+$ cation become more and more violent and display an overt disordered state as the temperature rising. Each disordered carbon atom and chlorine atom split into two nearby locations, with the occupation coefficient of 0.5. The disordered $[CEMP]^+$ cation is just like a rocking chair as in Fig. 2d. Nevertheless, the linear inorganic chain remains an ordered state without visible changes, As in Fig. 2e, this unique inorganic chain is formed by Br^- and $[SCN]^-$ connected to the shared metal atom Cd^{II} respectively, constituting a unique side-by-side structure. In short, the structure of HTP has overt distinction compared with LTP, which indicates that the internal mechanism of phase transition. The movement of $[CEMP]^+$ cation is the main driving force of phase transition.

In general, structural changes always in the form of the dielectric abnormality near the phase transformation temperature. Based on that, Fig. 3a shows the changing trend of the value of the real part at 1 MHz. In the heating model, the dielectric constant (ε') almost remains at a platform of ~4.5 with a slight rise as the temperature increases, which is on half of the low dielectric state (LTP, switch "off"). Abruptly, a steep step-like anomaly appears at around 320 K, and the dielectric constant rises significantly and rapidly to 7.5 correspondings to the high dielectric state (HTP, switch "on"). As in the cooling model, the value of ε' rapidly drops from 6.5 to 5 with a corresponding anomaly appeared when the temperature is cooling down to 305 K. The process above shows a reversible switchable phase transition in the process of heating and cooling. There is also obvious thermal hysteresis of 20 K in the dielectric diagram, which is consistent with DSC results.

The overt temperature hysteresis in the heating and cooling model would ascribe to the cationic apparent chair-rocking motion. It is noteworthy that the dielectric response can be rapidly tuned between high and low dielectric states, which indicates that the material would become a candidate for a molecular dielectric switch. Besides, Fig. 3b shows the dielectric constant variation under different frequencies from 500 KHz to 1 MHz when heating. There are apparent dielectric anomalies at a low frequency while the extent of change gradually decreases as

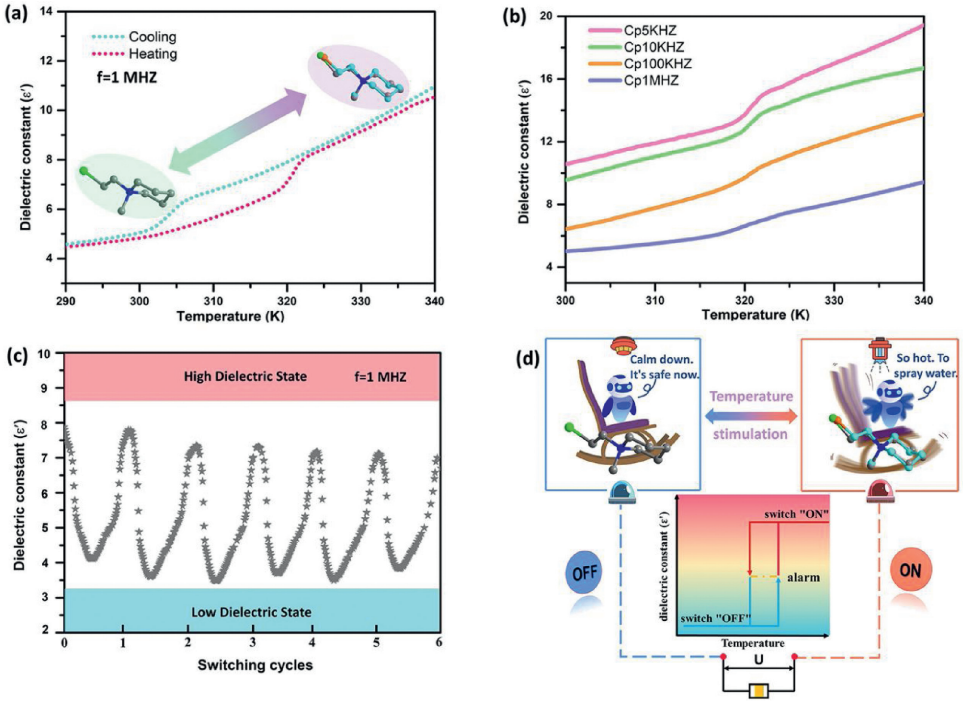

Fig. 3. (a) Temperature-dependence curves of the real part (ε') of **1** measured in the pressed-powder pellet at 1 MHz upon heating and cooling. (b) The dielectric constant (ε') of pressed-powder pellet for **1** at 5 kHz, 10 kHz, 100 kHz and 1 MHz in heating mode. (c) The recoverable switching of the dielectric effect of the pressed powder pellet for **1** (One cycle took 800 s). (d) Simulated application of dielectric switch for **1** with excellent thermal sensitivity.

the frequency rise, which means the permittivity of the crystal of **1** is sensitive to external frequencies with no relaxation. This interesting phenomenon implies that the compound **1** can be made in a new-type molecular dielectric switch with a function of delaying buffer alarm.

Intelligent thermal material combined with dielectric responsiveness based on molecules has the ability to perform "on-off" conversion by receiving and decoding thermal/electrical signals near the phase transition temperature, which is integrated into a single-molecule module. The dielectric switching cycle measurement of the pressed-powder pellet was executed to bear out the reversibility of dielectric switching as in Fig. 3c. The strength and the magnitude of the dielectric single remain almost the same as the initial value with stable dielectric signals after running several cycles, which verifies remarkably dielectric stability. Therefore, the simulated application of **1** (Fig. 3d) was designed to apply for a temperature sensor switch and memory devices. This is one of the research characteristics of condensed matter physics. When the temperature reaches to phase transition point, the switch would be turned on automatically. Correspondingly, the switch would be turned off when below the temperature stimulus point, which is like an intelligent robot operating the process above.

In work, we put forward a novel compound with unusual high-temperature reversible dielectric switching behavior. By replacing hydrogen with flexible groups, the steric hindrance is increased, and then the energy barrier is raised, which leads to a high-temperature reversible phase transition. Through the structural characterization, the phase transition is mainly caused by the unusual chair-rocking motion of $[CEMP]^+$ cation, which makes **1** exhibit excellent anisotropy and stable dielectric switching characteristics. Meanwhile, it is a fantastic strategy to dope $[SCN]^-$ ions in perovskite compounds to trigger phase transition and higher T_c of the dielectric switch. The new finding provides a new direction to enrich new applications and design ideas of perovskite materials.

Declaration of competing interest

The authors declare that they have no known competing financial interests or personal relationships that could have appeared to influence the work reported in this paper.

Acknowledgments

This work was supported by the National Natural Science Foundation of China (No. 21991141), Natural Science Foundation of Zhejiang Province (No. LZ20B010001) and Zhejiang Normal University for financial support.

Appendix A. Supplementary data

Supplementary material related to this article can be found, in the online version, at doi:https://doi.org/10.1016/j.cclet.2021.02.040.

References

[1] H. Pan, F. Li, Y. Liu, et al., Science 365 (2019) 578–582.
[2] P.P. Shi, S.Q. Lu, X.J. Song, et al., J. Am. Chem. Soc. 141 (2019) 18334–18340.
[3] Z.X. Zhang, H.Y. Zhang, W. Zhang, et al., J. Am. Chem. Soc. 142 (2020) 17787–17794.
[4] H.Y. Zhang, X.G. Chen, Z.X. Zhang, et al., Adv. Mater. 32 (2020) 2005213.
[5] C. Shi, H. Yu, Q.W. Wang, et al., Angew. Chem. Int. Ed. 59 (2020) 167–171.
[6] J. Dong, Y. Lu, X.X. Tian, et al., Small 16 (2020) 2003824.
[7] W.C. Zhang, M.C. Hong, J.H. Luo, Angew. Chem. Int. Ed. 59 (2020) 9305–9308.
[8] L.J. Ji, S.J. Sun, Y. Qin, K. Li, W. Li, Coord. Chem. Rev. 391 (2019) 15–29.
[9] F. Jiang, D. Yang, Y. Jiang, et al., J. Am. Chem. Soc. 140 (2018) 1019–1027.
[10] Z.X. Zhang, C.Y. Su, J.X. Gao, T. Zhang, D.W. Fu, Sci. China Mater. 64 (2020) 706–716.
[11] J.M. Shi, W. Aftab, Z.B. Liang, et al., J. Mater. Chem. A 8 (2020) 20133–20140.
[12] W. Li, L.J. Ji, Science 361 (2018) 132.
[13] X.G. Chen, X.J. Song, Z.X. Zhang, et al., J. Am. Chem. Soc. 142 (2020) 1077–1082.
[14] X. Zhang, L. Li, Z. Sun, J. Luo, Chem. Soc. Rev. 48 (2019) 517–539.
[15] Y. Xue, Z. Zhang, P. Shi, et al., Chin. Chem. Lett. 32 (2020) 539–542.
[16] Y. Zhang, H.Y. Ye, H.L. Cai, et al., Adv. Mater. 26 (2014) 4515–4520.
[17] X.G. Chen, X.J. Song, Z.X. Zhang, et al., J. Am. Chem. Soc. 142 (2020) 10212–10218.
[18] H.Y. Zhang, X.J. Song, H. Cheng, et al., J. Am. Chem. Soc. 142 (2020) 4604–4608.
[19] W.W. Cui, X. Zhang, C.I. Pearce, et al., Environ. Sci. Technol. 53 (2019) 11043–11055.
[20] S. Horiuchi, S. Ishibashi, S. Inada, S. Aoyagi, Cryst. Growth Des. 19 (2019) 328–335.
[21] X.H. Zhao, X.C. Huang, S.L. Zhang, et al., J. Am. Chem. Soc. 135 (2013) 16006–16009.
[22] Y. Tian, S. Shen, J. Cong, et al., J. Am. Chem. Soc. 138 (2016) 782–785.
[23] Y. Chen, B. Li, W. Huang, D. Gao, Z. Liang, Chem. Commun. 51 (2015) 11997–11999.
[24] T. Zhang, L. Chu, Z. Zhang, et al., Sci. China Mater. 63 (2020) 2281–2288.
[25] S.Y. Zhang, X. Shu, Y. Zeng, et al., Nat. Commun. 11 (2020) 2752.
[26] H. Liu, H.Y. Zhang, X.G. Chen, R.G. Xiong, J. Am. Chem. Soc. 142 (2020) 15205–15218.
[27] Y.F. Xie, Y. Ai, Y.L. Zeng, et al., J. Am. Chem. Soc. 142 (2020) 12486–12492.
[28] J. Harada, N. Yoneyama, S. Yokokura, et al., J. Am. Chem. Soc. 140 (2018) 346–354.
[29] W.Q. Liao, Y.Y. Tang, P.F. Li, Y.M. You, R.G. Xiong, J. Am. Chem. Soc. 140 (2018) 3975–3980.
[30] Y. Zhang, X.J. Song, Z.X. Zhang, D.W. Fu, R.G. Xiong, Matter 2 (2020) 697–710.
[31] L.L. Chu, T. Zhang, Y.F. Gao, et al., Chem. Mater. 32 (2020) 6968–6974.
[32] D.W. Fu, J.X. Gao, W.H. He, et al., Angew. Chem. Int. Ed. 59 (2020) 17477–17481.
[33] J.X. Gao, W.Y. Zhang, Z.G. Wu, Y.X. Zheng, D.W. Fu, J. Am. Chem. Soc. 142 (2020) 4756–4761.
[34] J. Harada, Y. Kawamura, Y. Takahashi, et al., J. Am. Chem. Soc. 141 (2019) 9349–9357.
[35] B. Huang, L.Y. Sun, S.S. Wang, et al., Chem. Commun. 53 (2017) 5764–5766.